Organic Electronics 13 (2012) 744–749

Contents lists available at SciVerse ScienceDirect

Organic Electronics

journal homepage: www.elsevier.com/locate/orgel

Energy level alignment in PCDTBT:$PC_{70}BM$ solar cells: Solution processed NiO_x for improved hole collection and efficiency

Erin L. Ratcliff [a,*], Jens Meyer [b], K. Xerxes Steirer [a], Neal R. Armstrong [a], Dana Olson [c], Antoine Kahn [b]

[a] Department of Chemistry and Biochemistry, University of Arizona, Tucson, AZ 85721, USA
[b] Department of Electrical Engineering, Princeton University, Princeton, NJ 08544, USA
[c] National Center for Photovoltaics, National Renewable Energy Laboratory, Golden, CO 80401, USA

ARTICLE INFO

Article history:
Received 22 November 2011
Received in revised form 20 January 2012
Accepted 21 January 2012
Available online 7 February 2012

Keywords:
Electronic structure
Photoemission spectroscopy
PCDTBT
Blend
Interface dipole
NiO_x

ABSTRACT

Solution-based NiO_x outperforms PEDOT:PSS in device performance and stability when used as a hole-collection layer in bulk-heterojunction (BHJ) solar cells formed with poly[*N*-9′-heptadecanyl-2,7-carbazole-alt-5,5-(4′,7′-di-2-thienyl-2′,1′,3′-benzothiadiazole) (PCDTBT) and $PC_{70}BM$. The origin of the enhancement is clarified by studying the interfacial energy level alignment between PCDTBT or the 1:4 blended heterojunctions and PEDOT:PSS or NiO_x using ultraviolet and inverse photoemission spectroscopies. The 1.6 eV electronic gap of PEDOT:PSS and energy level alignment with the BHJ result in poor hole selectivity of PEDOT:PSS and allows electron recombination at the PEDOT:PSS/BHJ interface. Conversely, the large band gap (3.7 eV) of NiO_x and interfacial dipole ($\geqslant$0.6 eV) with the organic active layer leads to a hole-selective interface. This interfacial dipole yields enhanced electron blocking properties by increasing the barrier to electron injection. The presence of such a strong dipole is predicted to further promote hole collection from the organic layer into the oxide, resulting in increased fill factor and short circuit current. An overall decrease in recombination is manifested in an increase in open circuit voltage and power conversion efficiency of the device on NiO_x versus PEDOT:PSS interlayers.

1. Introduction

Interfacial phenomena play key roles in the overall power conversion efficiency (PCE) of organic photovoltaics (OPV). In particular, the electronic and molecular structures of the organic/organic′ or donor/acceptor (D:A) interface dominate exciton dissociation and charge transfer within the blend and control open circuit voltage (V_{OC}) and short circuit current (J_{SC}) in both planar and bulk heterojunction (BHJ) devices. In this context, significant effort has been focused on the optimization and improvement of the poly-3-hexylthiophene:[6,6]-phenyl-C_{61}-butyric acid methyl ester (P3HT:$PC_{60}BM$) heterojunction, with maximum achieved PCE of ~4–5% [1]. The overall PCE of these devices is limited by two dominating factors. The first is a limitation attributed to the relatively high electronic band gap of P3HT (~2.5 eV) [2], which prevents photoconversion of the full solar spectrum and limits J_{SC}. The second limitation is the energetic alignment between the polymer (D) and the fullerene (A), which restricts the V_{OC} to ~0.6 V. Recent reports on BHJs constructed from the D:A poly[*N*-9′-heptadecanyl-2,7-carbazole-alt-5,5-(4′,7′-di-2-thienyl-2′,1′,3′-benzothiadiazole) (PCDTBT):$PC_{60}BM$ BHJ indicate an increase of V_{OC} to 0.9 V [3] as well as increased air and thermal stability of the polymer [4]. BHJs containing PCDTBT and [6,6]-phenylC_{71} butyric acid methyl ester ($PC_{70}BM$) have demonstrated internal quantum efficiencies close to 100%, with overall PCEs above 6% [5]. The improvement in the efficiency over the P3HT:$PC_{60}BM$ heterojunction has been attributed to an increased energy offset between the highest occupied molecular orbital (HOMO) of the donor polymer PCDTBT

* Corresponding author.
E-mail address: ratcliff@email.arizona.edu (E.L. Ratcliff).

1566-1199/$ - see front matter © 2012 Elsevier B.V. All rights reserved.
doi:10.1016/j.orgel.2012.01.022

Table 1
Device characteristics for PCDTBT:$PC_{70}BM$ BHJ OPVs with NiO_x and PEDOT:PSS HTLs.

HTL	J_{SC} (mA cm^{-2})	V_{OC} (V)	FF	PCE (%)
NiO_x	−11.5 (±0.4)	0.88 (±0.01)	0.65 (±0.01)	6.7 (±0.1)
PEDOT:PSS	−11.1 (±0.1)	0.85 (±0.01)	0.60 (±0.01)	5.7 (±0.1)

and the lowest unoccupied molecular orbital (LUMO) of the acceptor $PC_{70}BM$ [6,7]. However, the energy gap of PCDTBT and the energy alignment at the PCDTBT:$PC_{70}BM$ interface have yet to be determined.

For BHJ devices, interlayers are required to prevent carrier recombination at the contact/blend interface and to preferentially collect one charge over the other (selective interlayer). Selectivity is typically achieved by introducing an interlayer with a large band gap at the electrode and has been shown to have a direct impact on V_{OC} and J_{SC} for PCDTBT devices [8–12]. Further improvements in efficiency have been demonstrated by changing the hole transport layer (HTL) of the device. As an example, an improvement of the PCE from 5.7% to 6.7% is achieved when replacing poly(3,4-ethylenedioxythiophene):poly(styrenesulfonate) PEDOT:PSS (on ITO) with solution processed NiO_x. The device characteristics are compared in Table 1 [10]; both J_{SC} and V_{OC} are found to increase upon substituting NiO_x for PEDOT:PSS. The enhancement is attributed to the increase in the HTL work function upon replacing the PEDOT:PSS (4.9 eV) with the oxygen-plasma treated NiO_x (5.3 eV). Yet, the energy level alignment between the donor and the acceptor within the blend, and between the blend and the selective interlayers cannot be predicted and must be measured independently. This manuscript presents direct measurements of these interface energetics using ultra-violet and inverse photoemission spectroscopy (UPS/IPES). Focus is placed on the energetics within the blend and interactions with two HTLs: PEDOT:PSS and NiO_x and reveals the strong effects that interfacial energy level alignment play in the formation of selective hole contacts.

2. Materials and methods

2.1. Substrate and HTLs

All films were deposited onto commercially patterned ITO (~10 Ω/sq, Thin Film Devices, Inc.) substrates after 5 min of ultrasonic cleaning in acetone followed by isopropyl alcohol. Substrates were plasma-cleaned immediately prior to HTL deposition in 0.8 Torr of O_2 at 155 W. Baytron P VP AI 4083 PEDOT:PSS was obtained from Covion and filtered through a 0.45 μm PTFE filter before use. Two coats of PEDOT:PSS were spin coated onto ITO at 6000 rpm and resulted in a 34 nm thick HTL in a normal device configuration, as measured by ellipsometry and stylus profilometry [10]. The NiO_x films were synthesized by spin-coating the diluted nickel ink at 4000 rpm for 60 s followed by annealing on a hot plate in air at 250 °C for 1 h, resulting in approximately 10 nm thick films as measured by ellipsometry and stylus profilometry [10]. After annealing, NiO_x interlayers were exposed to O_2-plasma treatment for 2 min at 155 W at 0.8 Torr.

2.2. Active layers

PCDTBT (Konarka) and $PC_{70}BM$ (Nano-C) were used as received. Anhydrous 1,2-dicholorbenzene (Aldrich) was purged with nitrogen to remove residual oxygen prior to use. Films of PCDTBT (1 mg/mL), $PC_{70}BM$ (10 mg/mL), and PCDTBT:$PC_{70}BM$ blend (1:4 ratio by weight; polymer at 1 mg/mL) were spun from 1,2-dichlorobenze solutions at 500 rpm for 10 min onto the PEDOT:PSS and post O_2-plas-

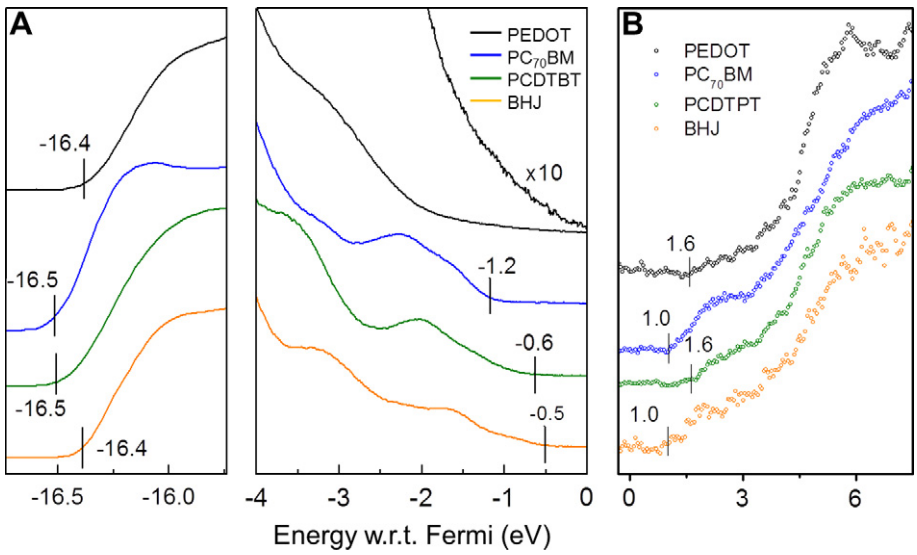

Fig. 1. (A) UPS spectra of PEDOT:PSS, $PC_{70}BM$, PCDTBT, and 1:4 PCDTBT:$PC_{70}BM$ BHJ spun on PEDOT:PSS. The left panel corresponds to the onset of photoemission. (B) IPES spectra of PEDOT:PSS and of the same films as in (A).

ma treated NiO_x interlayers, as previously described [10,13,14]. Active layers were exposed briefly to air prior to loading into the ultra-high vacuum (UHV) chamber for analysis.

2.3. Spectroscopy

UPS and IPES measurements were carried out in an UHV chamber with base pressure $\sim 10^{-10}$ Torr. He I (21.22 eV) radiation was used in UPS, with an experimental resolution of 0.15 eV. IPES was operated in the isochromat mode with a resolution of 0.45 eV [15]. The Fermi level reference was established for both UPS and IPES measurements on a freshly evaporated Au surface.

3. Results and discussion

The UPS and IPES spectra of a film of PEDOT:PSS and of $PC_{70}BM$, PCDTBT, and PCDTBT:$PC_{70}BM$ (1:4 ratio by weight) thin films on PEDOT:PSS are shown in Fig. 1A and B. Vertical tick marks denote the onset of photoemission for calculation of the sample work function (left panel Fig. 1A) and the edges of filled (right panel Fig. 1A) and empty states (Fig. 1B) that define the position of the HOMO and LUMO edges. The resulting energy diagrams with molecular level alignments of the materials on PEDOT:PSS are shown in Fig. 2.

The bare PEDOT:PSS exhibits a work function of 4.9 eV, as deduced from the onset of photoemission (left panel, Fig. 1A). The UPS spectrum is in good agreement with those reported by Hwang et al. and Xing et al., showing an onset of strong density of states about 2 eV below the Fermi level [16,17]. This energy difference results from the fact that the p-doped PEDOT core is covered by a 2–4 nm thick PSS shell, which has a higher energy gap, larger ionization energy (IE) and smaller electron affinity (EA) than the doped PEDOT. A weak intensity corresponding to the top PEDOT valence states tailing to the Fermi level is observed through the PSS layer, as shown in the 10-fold magnification of the UPS spectrum [16]. The EA of the film is 3.3 eV, deduced from the vacuum level measured in UPS

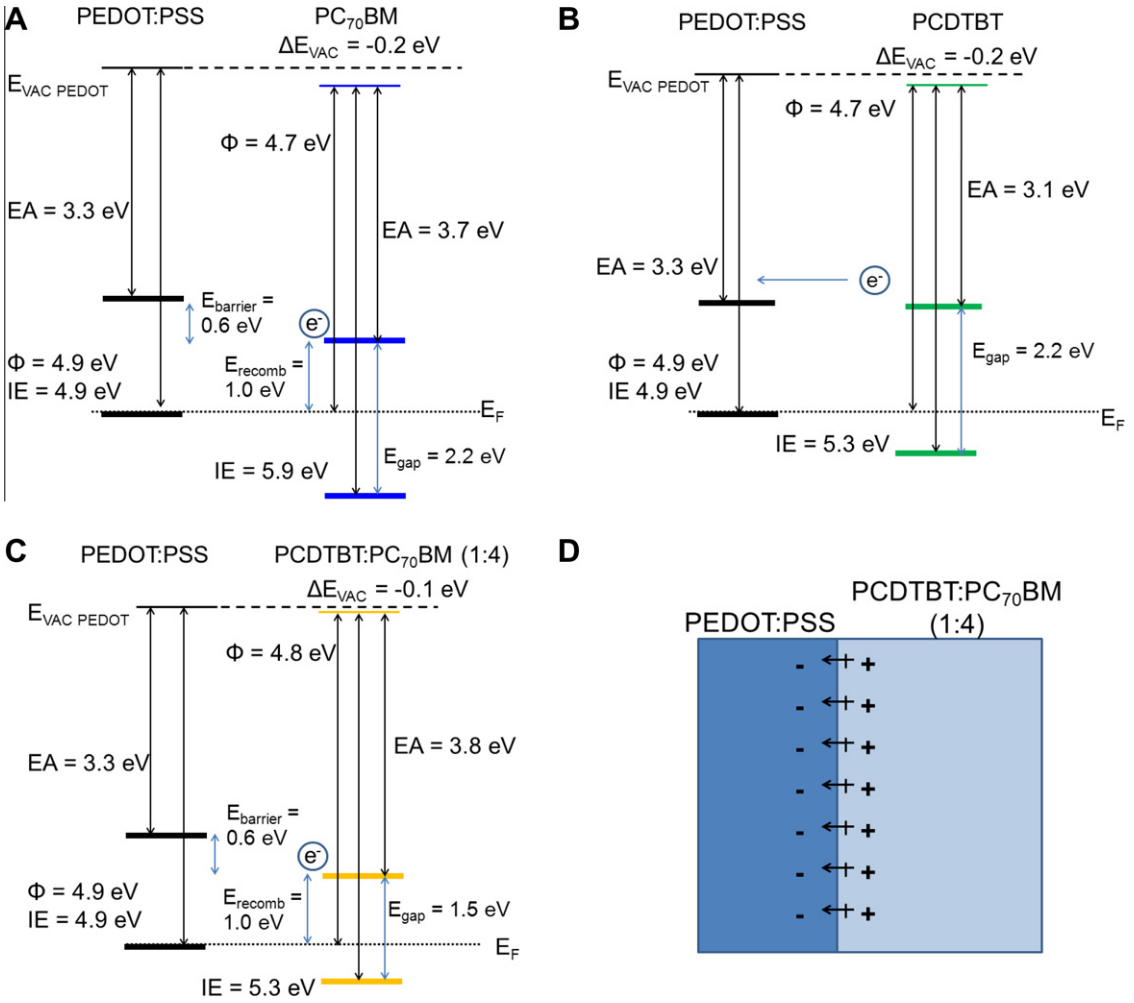

Fig. 2. Energy level alignment of thin films from (A) PC70BM, (B) PCDTBT, (C) 1:4 PCDTBT:$PC_{70}BM$ BHJ on PEDOT:PSS and (D) a dipole schematic of PEDOT:PSS/BHJ interface.

and the edge of the empty states measured in IPES (Fig. 1B). This relatively large EA, or low lying LUMO, of PEDOT:PSS may result in facile injection of electrons from the LUMO of the donor or acceptor directly into the LUMO of PEDOT:PSS, resulting in undesirable recombination directly at the interlayer interface (Fig. 2). Therefore, any electron blocking capabilities of PEDOT:PSS would need to arise predominantly from dipole shifts with subsequent organic layers to increase the LUMO offset.

The onset of photoemission (Fig. 1A) shows that there is a very small vacuum level shift ($\leqslant$0.2 eV) between PEDOT:PSS and the organic active layer components. Therefore, there is only a small interface dipole between (i) the HTL and the components of the BHJ and (ii) the HTL and the BHJ itself (Fig. 2). On PEDOT:PSS, the IE and EA of $PC_{70}BM$ are 5.9 eV and 3.7 eV, respectively, yielding an electronic gap of 2.2 eV. The energy diagram (Fig. 2A) derived from the data of Fig. 1 indicates that the energy for surface recombination (E_{recomb}) between the $PC_{70}BM$ LUMO and the PEDOT HOMO is 1.0 eV. This energy is the driving force for annihilation of an electron on the fullerene by a hole in the interlayer [18,19]. There is a 0.6 eV barrier to electron injection from the $PC_{70}BM$ into the PEDOT:PSS, indicating some degree of electron blocking character. The IE of the PCDTBT on PEDOT:PSS is 5.3 eV, with the HOMO edge located approximately 0.5 eV below the Fermi level, consistent with previous reports [20]. The onset of the PCDTBT LUMO (Fig. 1B) is at 1.6 eV above the Fermi level (EA = 3.1 eV), resulting in an electronic band gap of 2.2 eV, slightly higher than the reported electrochemical gap of $\sim$1.85 eV [6,21]. However, the electronic gap of the PCDTBT (2.2 eV) is lower than the reported electronic gap for P3HT (2.5 eV) [2]. This difference in gap has been suggested to enhance photocurrent in PCDTBT-based BHJs over P3HT-based BHJs [6,7].

The small dipole shift between PCDTBT and PEDOT:PSS ($-$0.2 eV) results in a fairly close alignment of the PCDTBT LUMO with the PEDOT:PSS LUMO, allowing relatively easy electron injection into the HTL interlayer and leading to a possible increase in rate of recombination at the interface (Fig. 2) [18,19]. Furthermore, the PCDTBT IE almost directly correlates with the blend IE (5.3 eV), consistent with findings by Wang et al. [22]. The $PC_{70}BM$ EA directly corresponds with the blend EA (3.8 eV), yielding a measured donor/acceptor band gap E_{gap} of 1.5 eV. The equivalence between the energetics of the individual components of the blend and of the blend itself indicates that there is only a minimal dipole between the donor and acceptor in the blend. This is in contrast with the two previously investigated cases of P3HT:$PC_{60}BM$ [2] and P3HT:ICBA [23], both of which exhibit 0.3–0.4 eV dipoles, and is due to the larger energy difference between the donor IE and acceptor EA. Guan et al. previously demonstrated that the electronic gap of the P3HT:$PC_{60}BM$ blend was 1.34 eV–1.46 eV [2]. The difference in the electronic gap when comparing the two blends correlates directly with the observed differences in V_{OC} (P3HT:$PC_{60}BM$ $V_{OC} \sim$ 0.6–0.65 V, PCDTBT:$PC_{70}BM$ $V_{OC} \sim$ 0.85–0.88 V). The electron injection barrier ($E_{barrier}$) from the LUMO of the blend into the PEDOT:PSS LUMO is only 0.6 eV, which may allow additional recombination current, reducing the V_{OC} when PEDOT:PSS is used as an interlayer [18,19].

A previous study of O_2-plasma treated, solution processed NiO_x interlayers determined that the near-surface region is composed of NiO, $Ni(OH)_2$, NiOOH, and water species [24]. Upon oxygen plasma treatment of the NiO_x interlayer, a strong dipole is formed at the interface due to the increase in NiOOH species, which increases the work function to 5.3 eV [24]. Because the surface chemistry of NiO_x may play an important role in determining the interfacial interactions with the organic active layer components, the band alignment was measured using UPS (Fig. 3). The corresponding energy band diagrams are shown in Fig. 4. Large vacuum level shifts are observed be-

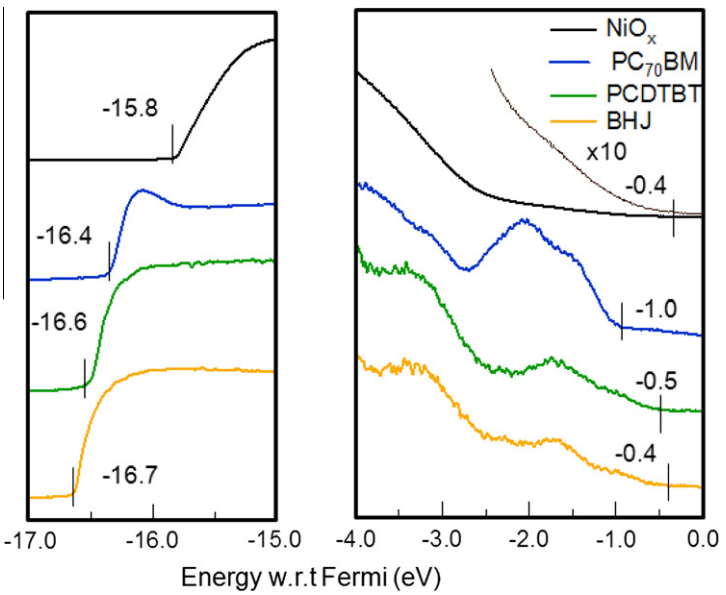

Fig. 3. UPS spectra of NiO_x, $PC_{70}BM$, PCDTBT, and 1:4 PCDTBT:$PC_{70}BM$ BHJ spun on NiO_x. The left panel corresponds to the onset of photoemission.

tween the three organic films and the oxide HTL compared to the same films on PEDOT:PSS. The magnitude of the vacuum level shift increases as the IE of the organic material decreases, which is to be expected as the HOMO of the organics must remain below the Fermi level of the NiO_x. Interestingly, there is a dipole shift ($\Delta E_{VAC} = -0.6$ eV) for the fullerene even though its IE and EA are significantly larger and smaller, respectively, than the NiO_x work function and charge transfer between the two materials is not expected. This large dipole is most likely due to the surface species on NiO_x and was observed previously for $PC_{60}BM$ on solution-processed NiO_x films [24].

The blend shows a very favorable energetic alignment with NiO_x (Fig. 4), as compared to the alignment of PEDOT:PSS (Fig. 2). The top of the oxide valence band and the HOMO of the blend are aligned, insuring barrier-less extraction of photo-generated holes at the NiO_x/PCDTBT:$PC_{70}BM$ interface. The NiO_x work function is high, leading to a large split-off of the quasi-Fermi levels for holes and electrons, and thus a large V_{OC}, under illumination. In addition, and unlike with PEDOT:PSS, the electronic gap of the NiO_x is 3.7 eV, placing the conduction band of the oxide at 2.2 eV above the LUMO of the blend, 0.8 eV higher than what is predicted by simple vacuum level alignment, and further enhancing the electron-blocking properties of the NiO_x. This is one of the key contribution to increasing V_{OC} (Table 1). The large dipole at the interface (Fig. 4D) is oriented in the same favorable direction for hole collection from organic to oxide as the dipole between the BHJ/PEDOT:PSS (Fig. 2D), but the dipole is larger in magnitude. This interface dipole is hypothesized to be a contributing factor to the observed increase in fill factor (FF) and J_{SC}.

The energy for surface recombination (E_{recomb}) is 1.6 eV, larger than in the previous case. This may result in a higher driving force for recombination of an electron from the fullerene with a hole in NiO_x, relative to PEDOT:PSS (E_{recomb} = 1.0 eV). However, the presence of the surface dipole at the interface appears to counter this presumed driving force, and help increase V_{OC}.

In summary, we have investigated the interfacial electronic structures of PCDTBT, $PC_{70}BM$, and a PCDTBT:$PC_{70}BM$ blend on PEDOT:PSS and NiO_x contact layers. We determined that the solid-state electronic gap of PCDTBT is 2.2 eV, which is larger than what was previously predicted

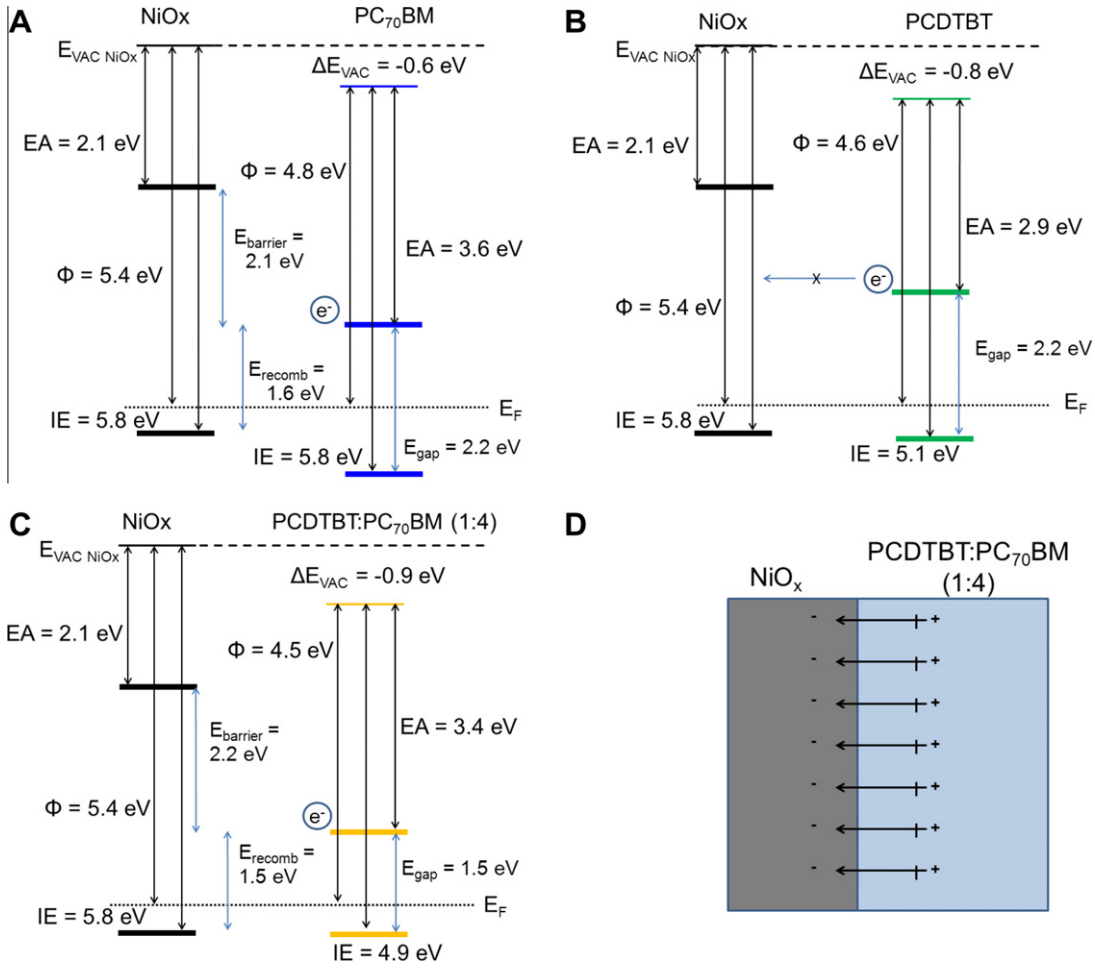

Fig. 4. Energy level alignment of thin films from (A) $PC_{70}BM$, (B) PCDTBT, (C) 1:4 PCDTBT:$PC_{70}BM$ BHJ on NiO_x and (D) a dipole schematic of NiO_x/BHJ interface.

by electrochemistry [6,21]. There is a minimal interfacial dipole between the donor and acceptor phases of the blend, and the IE and EA of the BHJ can be estimated from the independent donor and acceptor band diagrams. The energy level alignment between the PCDTBT:$PC_{70}BM$ blend and the underlying HTL is found to depend on the HTL, with a large interfacial dipole on NiO_x and a much smaller dipole on the lower work function PEDOT:PSS. The large band gap of NiO_x coupled with the electronic structure of the NiO_x/blend interface suggests that the oxide constitutes an excellent barrier to electron recombination at the electrode, and thus contributes to increasing V_{OC}. The improved FF and J_{SC} suggest that the orientation and magnitude of the interfacial dipole at the NiO_x/BHJ interface also enhances the device performance.

Acknowledgments

We would like to thank Konarka for providing the polymer PCDTBT. This research was supported as part of the Center for Interface Science: Solar Electric Materials, an Energy Frontier Research Center funded the U.S. Department of Energy, Office of Science, Office of Basic Energy Sciences, under Award Number DE-SC0001084 (NRA, ELR, KXS, DCO), NSF DMR-1005892 (AK), and the Deutsche Forschungsgemeinschaft (DFG) postdoctoral fellowship program (JM).

References

[1] G. Li, V. Shrotriya, J. Huang, Y. Yao, T. Moriarty, K. Emery, Y. Yang, Nature Materials 4 (2005) 864–868.
[2] Z.-L. Guan, J.B. Kim, H. Wang, C. Jaye, D.A. Fischer, Y.-L. Loo, A. Kahn, Organic Electronics 11 (2010) 1779–1785.
[3] T.Y. Chu, S. Alem, P.G. Verly, S. Wakim, J.P. Lu, Y. Tao, S. Beaupre, M. Leclerc, F. Belanger, D. Desilets, S. Rodman, D. Waller, R. Gaudiana, Applied Physics Letters 95 (2009).
[4] S. Cho, J.H. Seo, S.H. Park, S. Beaupre, M. Leclerc, A.J. Heeger, Advanced Materials 22 (2010) 1253–1257.
[5] S.H. Park, A. Roy, S. Beaupre, S. Cho, N. Coates, J.S. Moon, D. Moses, M. Leclerc, K. Lee, A.J. Heeger, Nature Photonics 3 (2009) 297–303.
[6] N. Blouin, A. Michaud, M. Leclerc, Advanced Materials 19 (2007) 2295–2300.
[7] N. Blouin, A. Michaud, D. Gendron, S. Wakim, E. Blair, R. Neagu-Plesu, M. Belletete, G. Durocher, Y. Tao, M. Leclerc, Journal of the American Chemical Society 130 (2008) 732–742.
[8] Y. Sun, C.J. Takacs, S.R. Cowan, J.H. Seo, X. Gong, A. Roy, A.J. Heeger, Advanced Materials 23 (2011) 2226–2230.
[9] Y.M. Sun, J.H. Seo, C.J. Takacs, J. Seifter, A.J. Heeger, Advanced Materials 23 (2011) 1679–1683.
[10] K.X. Steirer, P.F. Ndione, N.E. Widjonarko, M.T. Lloyd, J. Meyer, E.L. Ratcliff, A. Kahn, N.R. Armstrong, C.J. Curtis, D.S. Ginley, J.J. Berry, D.C. Olson, Advanced Energy Materials 1 (2011) 813–820.
[11] E.L. Ratcliff, B. Zacher, N.R. Armstrong, The Journal of Physical Chemistry Letters 2 (2011) 1337–1350.
[12] R. Steim, F.R. Kogler, C.J. Brabec, Journal of Materials Chemistry 20 (2010) 2499–2512.
[13] K.X. Steirer, J.P. Chesin, N.E. Widjonarko, J.J. Berry, A. Miedaner, D.S. Ginley, D.C. Olson, Organic Electronics 11 (2010) 1414–1418.
[14] K.X. Steirer, N.E. Widjonarko, A.K. Sigdel, M.T. Lloyd, D.S. Ginley, D.C. Olson, J.J. Berry, Optimization of organic photovoltaic devices using tuned mixed metal oxide contact layers, in: Photovoltaic Specialists Conference (PVSC), 2010, 35th IEEE, pp. 000102-000104.
[15] C.I. Wu, Y. Hirose, H. Sirringhaus, A. Kahn, Chemical Physics Letters 272 (1997) 43–47.
[16] J. Hwang, F. Amy, A. Kahn, Organic Electronics 7 (2006) 387–396.
[17] K.Z. Xing, M. Fahlman, X.W. Chen, O. Inganäs, W.R. Salaneck, Synthetic Metals 89 (1997) 161–165.
[18] A. Wagenpfahl, C. Deibel, V. Dyakonov, IEEE Journal of Selected Topics in Quantum Electronics 16 (2010) 1759–1763.
[19] A. Wagenpfahl, D. Rauh, M. Binder, C. Deibel, V. Dyakonov, Physical Review B 82 (2010).
[20] J.H. Seo, S. Cho, M. Leclerc, A.J. Heeger, Chemical Physics Letters 503 (2011) 101–104.
[21] S. Wakim, S. Beaupre, N. Blouin, B.R. Aich, S. Rodman, R. Gaudiana, Y. Tao, M. Leclerc, Journal of Materials Chemistry 19 (2009) 5351–5358.
[22] D.H. Wang, K.H. Park, J.H. Seo, J. Seifter, J.H. Jeon, J.K. Kim, J.H. Park, O.O. Park, A.J. Heeger, Advanced Energy Materials 1 (2011) 766–770.
[23] Z.-L. Guan, J.B. Kim, Y.-L. Loo, A. Kahn, Journal of Applied Physics 110 (2011) 043719.
[24] E.L. Ratcliff, J. Meyer, K.X. Steirer, A. Garcia, J.J. Berry, D.S. Ginley, D.C. Olson, A. Kahn, N.R. Armstrong, Chemistry of Materials 23 (2011) 4988–5000.